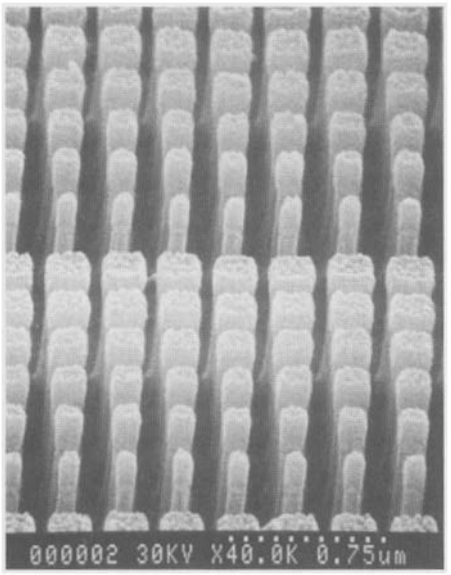

Lalanne Figure 1. SEM of a blazed-binary grating composed of subwavelength pillars etched in a TiO_2 film deposited on a glass substrate. The horizontal period (or sampling period) is equal to 272 nm and the period in the perpendicular direction is 1.9 μm. The grating depth is ≈816 nm and the maximum pillar aspect-ratio is ≈8.8.

taining high diffraction efficiency with large deflection angles is a challenge in design and fabrication of tomorrow's DOEs.

We have developed methods for the synthesis and fabrication of DOEs, called "blazed-binary" DOEs hereafter, which substantially outperform conventional blazed-échelette DOEs in the resonance domain. In our elements, each period (or zone) is composed of binary nano-pillars arranged on a square subwavelength grid and etched in a dielectric material (see Fig. 1).

By monitoring the local fraction of matter removed, we implement continuous phase delays and obtain strong blazing effects. The design exploits the analogy between subwavelength gratings and artificial dielectric materials.[2] The analogy is accurate when the distance between the subwavelength period of the square grid is smaller than some structural cut-off related to wave propagation in the nano-pillar region.[3]

Only one lithographic step is necessary for the fabrication. The process involves electron-beam lithography in a polymethyl methacrylate film, lift-off with an intermediate Nickel layer, and reactive ion etching of a TiO_2 film evaporated on a glass substrate.[4] The lift-off technique is used to enhance the selectivity and the fidelity of the pattern transfer during the etching.

Two binary-blazed DOEs with square-grid periods smaller than the structural cut-off have been designed, fabricated, and tested. The first one, a 3 λ-period (20° deflection in air) blazed-binary grating, is shown in Figure 1. For unpolarized light at 633 nm, the experimental diffraction efficiency in the transmitted first-order is 82%, a value 6% below theory. The grating behavior is nearly independent on polarization; the first-order efficiencies are 80% and 84% for TE and TM polarizations, respectively. As a matter of comparison, the maximum theoretical diffraction efficiency achieved by a transmission échelette grating in glass blazed in the first-order with a 3λ-period is 66.5%. Our second DOE is a 20° off-axis diffractive lens with a focal length of 400 μm, and a square pupil of 200 × 200 μm^2. The minimum and maximum zone widths are 1.91 λ and 8.83 λ, respectively, and half of the lens area is concerned with zone widths smaller than 2.8 λ. When measured with a vertical-cavity-surface-emitting laser emitting a Gaussian beam circularly polarized at 860 nm, a first-order diffraction efficiency of 80% is obtained. In addition to efficiency, the inspection of the point-spread function reveals a good operation.

Acknowledgment

This work was supported by the European Community under the RODCI Mel-Ari programme. The authors are grateful to Jean Landreau and Alain Carenco (Centre National des Etudes de Télécommunications; CNET-Bagneux) for coating the TiO_2 films.

References

1. T. Hessler *et al.*, "Analysis and optimization of fabrication of continuous-relief diffractive optical elements," Appl. Opt. **37,** 4069–4079 (1998).
2. W. Stork *et al.*, "Artificial distributed-index media fabricated by zero-order gratings," Opt. Lett. **16,** 1921–1923 (1991).
3. P. Lalanne *et al.*, "Blazed-binary subwavelength gratings with efficiencies larger than those of conventional échelette gratings," Opt. Lett. **23,** 1081–1083 (1998).
4. S. Astilean *et al.*, "High efficiency subwavelength element patterned in a high-refractive-index material for 633 nm," Opt. Lett. **23,** 552–554 (1998).

Gaussian Wave Packets in Resonant Diffraction Gratings

Frank Schreier, Martin Schmitz, and Olof Bryngdahl, Physics Dept., Univ. of Essen, Essen, Germany.

Resonant diffraction gratings are frequently used as convenient and flexible wavelength filters since they offer a reflectance >99% for their central wavelength, whereas far off the central wavelength the reflectance can fall below 1%. The central wavelength can be adjusted by the choice of the angle of incidence, and the FWHM of the filter can be fixed over a wide range during the design process. Resonance effects occur due to the coupling of the incident wave to guided modes supported by a waveguide layer of the structure. Numerical considerations concerning resonant gratings are usually carried out under the assumption of an incident plane wave.

We numerically investigated the spatial behavior of a Gaussian beam[1] and the temporal behavior of a Gaussian pulse[2] incident on a diffractive structure under resonance conditions. Two different geometries are considered: a waveguide grating, where the relative permittivity of a guiding layer exhibits a sinusoidal modulation (see Fig. 1a, page 22), and a waveguide structure, where the waveguide layer is separated from a substrate by a gap layer with low relative permittivity (see Fig. 1b). The coupling mechanism that results in a resonance is different for the two geometries presented. It was demonstrated that in both geometries a beam may undergo a lateral displacement, similar to the Goos-Hänchen-shift, which can grow as large as the order of the beam width; for a beam having a half-width of 9.3 mm, a lateral displacement of 5.2 mm has been observed. This displacement is several orders of magnitude larger compared to the Goos-Hänchen-shift. Additionally it is shown that only the given beam width imposes a restriction on the maximum achievable displacement.

A close analogy between the spatial and the temporal properties is established, giving rise to analogous effects in the time domain. The lateral displacement corresponds to a temporal delay. Under resonance conditions a pulse incident on the structures can be subject to a temporal delay that can reach the order of the pulse duration; for a pulse of 100 ps duration a delay of 40 ps can be achieved. Moreover, negative delays are possible: the maximum of intensity of a diffracted pulse can advance the maximum of intensity of the incident pulse. For this effect to occur, the diffraction efficiency has to be small; otherwise, the effect will result in a violation of causality.

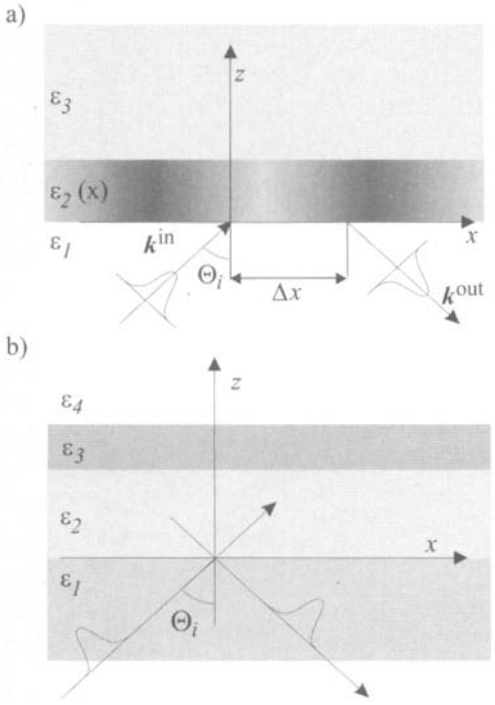

Schreier Figure 1. Resonant diffractive structures. (a) Waveguide grating with a period equal to 0.8 λ. (b) Single-mode waveguide structure.

For both structures, geometrical or material parameters were found that allowed control of the maximum displacement and delay over a wide range. It is expected that the effects described can find numerous applications, *e.g.*, integrated optics.

References

1. F. Schreier *et al.*, "Beam displacement at diffractive structures under resonance conditions," Opt. Lett. **23,** 576–578 (1998).
2. F. Schreier *et al.*, "Pulse delay at diffractive structures under resonance conditions," Opt. Lett. **23,** 1337–1339 (1998).

INTERFEROMETRY

Temporal Speckle Pattern Interferometry

C. Joenathan, Dept. of Physics and Applied Optics, Rose-Hulman Institute of Tech, Terre Haute, IN; P. Haible and H.J. Tiziani, Universität Stuttgart, Institut für Technische Optik, Stuttgart, Germany.

In recent years, speckle techniques have been propelled from scientific to industrial environments due to rapid advancements in computer technology and its peripherals. In many ways, the limited use of speckle techniques is set by its relatively high sensitivity, thereby only displacements in the range of 5–6 μm can be measured. Recent developments to record the temporal fluctuation of speckles rather than changes in spatial distribution have rendered the possibility of measuring large displacements over 100 μm with almost the same accuracy as using phase shifting techniques.

In conventional speckle interferometric techniques an initial frame with the object in its undisturbed state is subtracted from the frame where the object is disturbed. Thereby spatial modulation of the speckle field is obtained (correlation fringes) where speckles that have not changed get eliminated and speckles that have changed generate a signal. To obtain better accuracy, phase shifting routines have been incorporated where accuracy in the range λ/20 is achieved.

A method proposed quite recently extracts information about the object deformation using temporal phase evaluation in a method called temporal speckle pattern interferometry (TSPI). The basic experimental setup is similar to conventional speckle interferometric techniques with sensitivity to in-plane or out-of-plane motion, but, in addition, rigid body movements are also measured. The light scattered from the object is imaged onto the sensor of a high-speed CCD camera, and interferes with a reference beam that is collinear to the object beam. A large number of frames (*e.g.*, 1024) of the speckle field is recorded over time as the object is being continuously deformed. Observing the intensity modulation, which is sinusoidal for a given speckle thus obtained, provides the temporal evolution related to the movement of the object at a corresponding point. The upper limit on the modulation frequency is set by the Nyquist criterion and is half the total number of frames used in the recording. By analyzing this time dependent signal, object deformation ranging from a few to a few hundreds of microns can be determined.

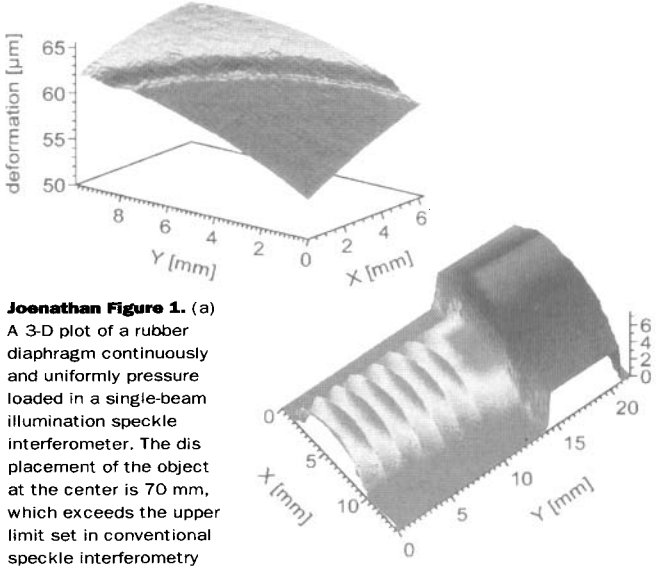

Joenathan Figure 1. (a) A 3-D plot of a rubber diaphragm continuously and uniformly pressure loaded in a single-beam illumination speckle interferometer. The displacement of the object at the center is 70 mm, which exceeds the upper limit set in conventional speckle interferometry using electronic processing. The accuracy of the deformation measurement is less than half the wavelength of light used in the experiment. The data was filtered with a spike removing filter of 5 × 5, which eliminated 0.1% of the pixels. The rubber diaphragm has a ridge that is harder than the other regions and therefore less deformed. The defect is pronounced in the plot showing the potential use of this method for NDT applications. (b) The shape of an M12 bolt measured by object rotation in a dual beam illumination speckle interferometer. The 3-D plot shown here is only spike filtered. The height of the object is measured with the new method of analysis with 1% accuracy. (See color image, page 15.)